

# An Adaptive Neuro-fuzzy Inference Scheme for Defect Detection and Classification of Solar Pv Cells

Ranganai Tawanda Moyo <sup>1</sup>, Mendon Dewa <sup>2</sup>, Héctor Felipe Mateo Romero <sup>3</sup>, Victor Alonso Gómez <sup>4</sup>, Jose Ignacio Morales Aragonés <sup>5</sup>, and Luis Hernández-Callejo <sup>6</sup>

<sup>1</sup> Department of Mechanical Engineering, Durban University of Technology, South Africa

<sup>2</sup> Department of Industrial Engineering, Durban University of Technology, South Africa

<sup>3</sup> Departamento Física de la Materia Condensada, Universidad de Valladolid, Spain

<sup>4,5</sup> Departamento de Física, Universidad de Valladolid, Spain

<sup>6</sup> Departamento Ingeniería Agrícola y Forestal, Universidad de Valladolid, Spain

moyoranganai@gmail.com, mendond@dut.ac.za, hectorfelipe.mateo@uva.es, victor.alonso.gomez@uva.es, joseignacio.morales@uva.es, luis.hernandez.callejo@uva.es

## ABSTRACT

*This research paper presents an innovative approach for defect detection and classification of solar photovoltaic (PV) cells using the adaptive neuro-fuzzy inference system (ANFIS) technique. As solar energy continues to be a vital component of the global renewable energy mix, ensuring the reliability and efficiency of PV systems is paramount. Detecting and classifying defects in PV cells are crucial steps toward ensuring optimal performance and longevity of solar panels. Traditional defect detection and classification methods often face challenges in providing precise and adaptable solutions to this complex problem. In this study the researchers pose an ANFIS-based scheme that combines the strengths of neural networks and fuzzy logic to accurately identify and classify various types of defects in solar PV cells. The adaptive learning mechanism of ANFIS enables the model to continuously adapt to changes in operating conditions ensuring robust and reliable defect detection capabilities. The ANFIS model was developed and implemented using MATLAB and a high predicting accuracy was achieved.*

**Index-words:** ANFIS, Fuzzy logic, PV cells, Defect detection and classification, MATLAB.

## I. INTRODUCTION

The global quest for renewable energy sources has propelled solar photovoltaic (PV) technology to the forefront of sustainable energy solutions [1]. As the demand for solar power escalates, the efficiency and reliability of PV modules become paramount. Solar panels are generally designed to have a lifespan of about 25 years [2]. However, the performance of solar panels is intricately linked to the quality and integrity of their individual PV cells. Defects in PV cells, such as micro-cracks, hotspots, and delamination, can significantly degrade the performance of solar panels, leading to reduced power output, shortened lifespan, and in severe cases, complete system failure [3]. Timely and accurate identification of these defects is indispensable to mitigate energy losses and ensure the sustained performance of solar PV systems.

Visual inspection, a traditional method of defect detection, involves human inspectors visually examining PV cells for any visible irregularities or flaws [4]. This method is relatively straightforward and cost-effective, providing a quick assessment of surface defects such as cracks, chips, or discolorations. Sadok et al. [5] conducted research on the assessment of PV modules' degradation based on visual inspection. In their conclusion, they deduced that the visual inspection technique is cost-effective and more suitable for defects that are visible to the bare eye. However, the visual inspection method is subjective and may overlook subtle defects that could impact the long-term performance of PV cells, making it less suitable for comprehensive quality control [6]. In contrast, automated optical inspection (AOI) systems represent a significant advancement in defect detection technology for PV cells [7]. AOI utilizes high-resolution cameras and sophisticated

image processing algorithms to analyze the surface of PV cells with precision and consistency. These systems can detect a wide range of defects, including microcracks, soldering defects, and variations in cell appearance. By automating the inspection process, AOI enhances efficiency and reduces the likelihood of human error, thus it improves the performance of PV modules as reported in [8]. However, the efficiency of AOI systems mainly depends on the image processing algorithms, therefore selecting the suitable algorithm is of prime importance. Non-destructive testing (NDT) methods also play a crucial role in detecting internal defects within PV cells that may not be visible to the naked eye [9]. Techniques such as electroluminescence (EL) imaging, infrared thermography, and ultrasonic testing allow inspectors to assess the structural integrity and performance of PV cells without causing damage. NDT methods are particularly valuable for identifying defects such as delamination, hotspots, internal cracks, or cell-to-cell interconnect issues that could compromise the overall module's reliability. NDT techniques have been utilized for defect detection of PV cells in the studies [10-12]. However, NDT methods are expensive and time-consuming, particularly when inspecting large volumes of solar cells. Electrical characterization techniques can also be employed to evaluate the electrical performance of PV cells and identify deviations from expected behavior [13]. These techniques include current-voltage (I-V) curve tracing, spectral response measurements, and capacitance-voltage (C-V) profiling. Inspectors can identify defects such as shunts, junction failures, or degradation due to environmental factors by analyzing electrical parameters such as efficiency, fill factor, and open-circuit voltage. The only challenge when using electrical characterization techniques is that one needs to measure the electrical values of every solar cell to see the deviation from expected values, which might not be practical in operational settings.

More recently, advancements in technology have led to the development of machine learning-based defect detection systems for PV cells [14]. These systems leverage artificial intelligence algorithms to analyze data from various sources, including optical images, electrical measurements, and historical performance data of PV cells. By learning patterns associated with known defects, these systems can detect anomalies and predict potential failures before they occur, enabling proactive maintenance and quality assurance in solar panels. Among the

innovative artificial intelligence approaches, the Adaptive Neuro-Fuzzy Inference System (ANFIS) is a promising avenue for defect detection and classification within solar PV cells [15]. ANFIS combines the adaptive learning capabilities of neural networks with the interpretability of fuzzy logic, offering a hybrid intelligent system capable of modeling intricate, non-linear systems. Its unique feature of providing transparent decision-making processes positions ANFIS as a viable solution to address the complexities inherent in defect detection tasks. Compared to other techniques, the ANFIS offers significant advancements in the detection and classification of defects in solar photovoltaic (PV) cells. It provides an adaptive mechanism that dynamically adjusts to varying defect types and environmental conditions. This results in higher classification accuracy and improved sensitivity to minor defects that might be overlooked by conventional methods. Additionally, the proposed technique does not need electrical measurements to detect and classify solar cell defects, which is a key benefit when assessing solar cells during operational settings. Thus, this research investigates and evaluates the efficacy of an adaptive neuro-fuzzy inference scheme tailored explicitly for defect detection and classification of solar PV cells. The ANFIS is implemented for defect detection and classification based on EL imaging.

## II. COMMON SOLAR PV CELL DEFECTS

Solar PV cell defects may arise from various stages of production, handling, installation, and operation of solar modules [7]. Here are some common types of defects found in solar PV cells.

### A. Snail Trails

A "snail trail" defect in solar cells refers to dark-colored, wavy lines or trails observed on the surface of crystalline silicon solar cells, resembling the tracks left by a snail [16]. These defects typically result from the migration of metal impurities, such as iron or copper, within the silicon material of the cell, which can occur during manufacturing or over the cell operational lifetime due to environmental factors. While snail trails themselves may not always directly impact the cell electrical performance, they can serve as sites for additional defect formation and contribute to localized degradation over time, potentially leading to increased electrical resistance,

reduced efficiency, or cell failure. **Figure 1** shows a snail trail defect in solar cells.

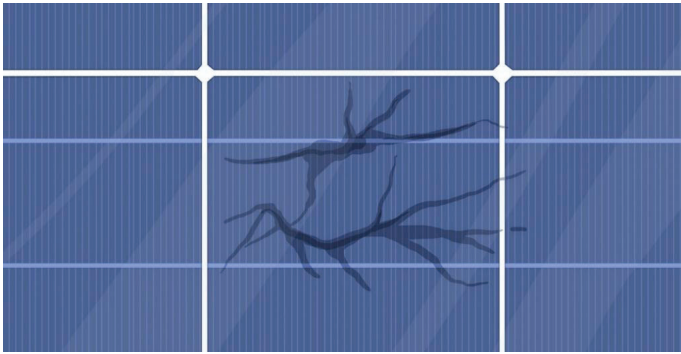


Fig. 1. A typical snail trail solar cell defect

### B. Cracks

Cracks in solar PV cells, as shown in **Figure 2**, can originate from various sources, including mechanical stress during manufacturing, transportation, or installation processes [17]. These stressors can cause fractures in the semiconductor material of the PV cell, such as crystalline silicon or thin-film layers. Cracks may also develop over time due to thermal cycling, expansion, and contraction of materials, or external impacts. Cracks can compromise the structural integrity of the cell, leading to electrical shorts, reduced efficiency, and increased susceptibility to environmental factors such as moisture ingress or corrosion. In severe cases, cracks can propagate through the entire cell, rendering it non-functional.

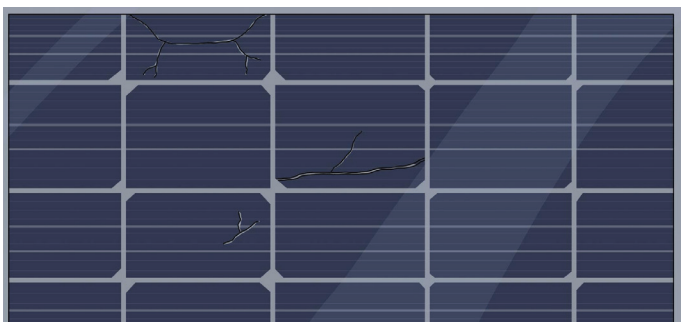


Fig. 2. Cracked solar cell

### C. Hotspots

Hotspots in solar PV modules occur when localized areas of the module experience higher temperatures than the surrounding regions [18]. Hotspots can arise from shading, mismatched cells, soiling, electrical faults, or bypass diode failures. When a portion of the module is shaded or experiences lower

illumination levels than the rest of the module, it can act as a current sink, causing reverse biasing of affected cells and localized heating. Hotspots can accelerate degradation processes, reduce module efficiency, and potentially lead to permanent damage or catastrophic failures if not addressed promptly. **Figure 3** shows hotspots in solar cells.

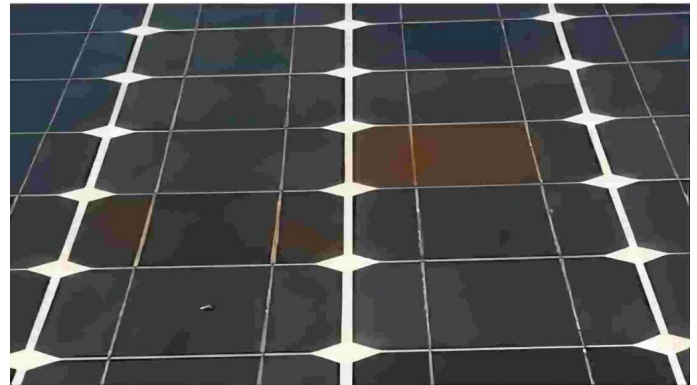


Fig. 3. Hotspots in solar cells

### D. Delamination

Delamination refers to the separation or detachment of layers within the PV module, typically involving the encapsulant layer that surrounds and protects the PV cells as shown in **Figure 4** [19]. Delamination can occur due to prolonged exposure to environmental factors such as moisture, UV radiation, temperature fluctuations, or mechanical stress. Moisture ingress between layers can weaken adhesive bonds, leading to separation, bubbling, or blistering of encapsulant layers. Delamination exposes the PV cells to environmental contaminants and accelerates degradation processes, reducing the module performance, reliability, and longevity.

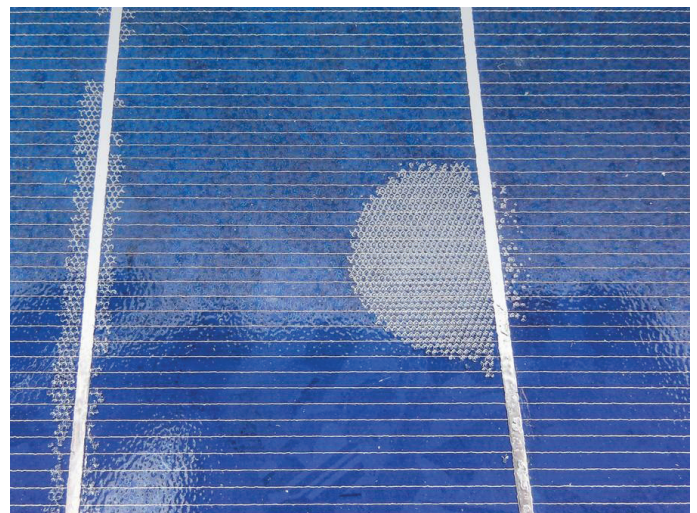


Fig. 4. Delamination defect in solar cells

### E. Soldering Defects

Soldering defects in solar PV cells often occur at the interconnections between individual cells, busbars, or ribbon connectors[20]. Poor soldering techniques, inadequate temperature control during soldering processes, or contamination of soldering materials can result in defective connections. Solder joints with inadequate bonding or excessive resistance can lead to increased electrical losses, localized heating, and hotspots within the module. Over time, soldering defects can worsen due to thermal cycling and mechanical stress, compromising the electrical integrity and reliability of the PV module. A soldering defect is shown in **Figure 5**.



Fig. 5. Soldering defects in solar cells

### F. Microcracks

Microcracks are small, often microscopic fractures that develop in solar PV cells due to mechanical stress, thermal cycling, or external impacts [21]. Microcracks may originate from manufacturing processes, handling, transportation, or installation activities. While individually small, microcracks can propagate and multiply over time, compromising the structural integrity and electrical performance of the PV module. Microcracks can serve as pathways for moisture ingress, leading to corrosion, delamination, or electrical degradation. They can also contribute to localized heating, hotspots, and increased susceptibility to mechanical failures or environmental stressors. **Figure 6** gives the EL image of small cracks in solar cells.

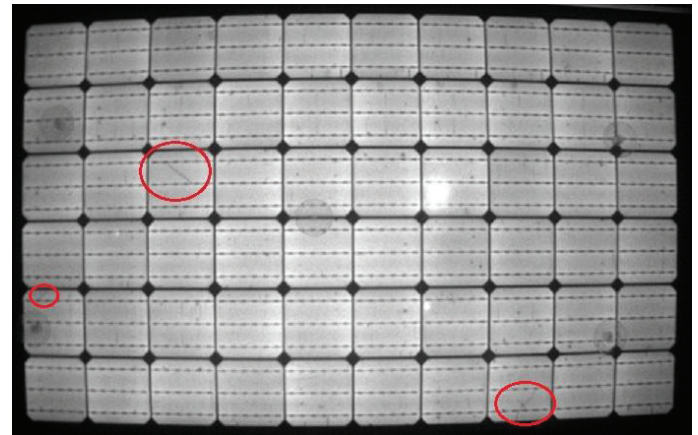


Fig. 6. EL image showing microcracks in solar cells

## III. ANFIS ARCHITECTURE

An Adaptive Neuro-Fuzzy Inference System (ANFIS) combines the strengths of neural networks and fuzzy logic to create a powerful tool for modeling complex systems and making accurate predictions [22]. The architecture of ANFIS comprises several layers, each responsible for different aspects of the learning process and inference. **Figure 7** shows the ANFIS architecture.

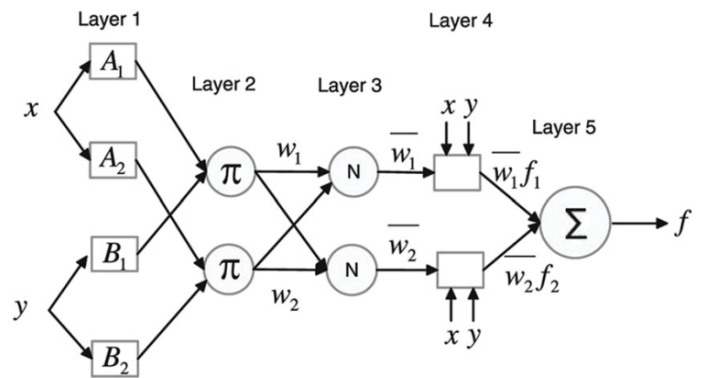


Fig. 7. A schematic diagram of the ANFIS architecture [23]

**Layer 1: Fuzzification Layer** - The first layer in an ANFIS architecture is the fuzzification layer, where crisp inputs are transformed into fuzzy sets. This layer consists of nodes known as membership functions, which represent the degree of membership of an input in different linguistic terms. The most common membership functions include triangular, Gaussian, and trapezoidal functions. Each input

is associated with several membership functions, which capture different aspects of its uncertainty and ambiguity.

**Layer 2: Rule Evaluation Layer** - In the rule evaluation layer, the fuzzified inputs are combined according to a set of predefined fuzzy rules. These rules encode expert knowledge or domain-specific information about the relationships between inputs and outputs. Typically, the rule base follows an “if-then” structure, where each rule specifies conditions under which a certain output should be activated. The activation level of each rule is determined by combining the degrees of membership of the input variables using fuzzy logic operators such as AND, OR, and NOT.

**Layer 3: Rule Consequent Layer** - The rule consequent layer calculates the contribution of each rule to the overall output of the system. Each rule has an associated consequence, which represents the output value predicted by that rule. The consequence is computed by combining the firing strengths of the input variables with adjustable parameters called consequent parameters. These parameters are typically optimized during the training process using techniques such as gradient descent or least squares estimation.

**Layer 4: Normalization Layer** - In the normalization layer, the firing strengths of the rules are normalized. Each node in this layer takes the firing strengths from the previous layer and computes the normalized firing strength by dividing each firing strength by the sum of all firing strengths. This normalization ensures that the sum of the normalized firing strengths equals one, making the system output more interpretable and stable.

**Layer 5: Defuzzification Layer** - The final layer in the ANFIS architecture is the defuzzification layer, where the fuzzy output obtained from the previous layer is converted back into a crisp output. This is achieved by aggregating the weighted outputs of all rules using methods such as centroid defuzzification or weighted averaging. The resulting crisp output represents the predicted value of the system based on the input variables and the learned fuzzy rules.

**Adaptive Learning Mechanism** - One of the key features of ANFIS is its ability to adaptively adjust its parameters based on training data. This is typically achieved using a combination of gradient

descent and backpropagation algorithms. During the training process, the consequent parameters of the fuzzy rules are adjusted to minimize the error between the predicted output and the actual output observed in the training data. Additionally, the shape and parameters of the membership functions can also be optimized to improve the model accuracy and generalization performance.

## A. Applications of the ANFIS Technique

The ANFIS represents a powerful fusion of artificial neural networks and fuzzy logic, offering a versatile approach to handling complex systems with both adaptability and interpretability. ANFIS models are particularly well-suited for applications where traditional techniques struggle to capture the intricacies of the underlying data [24]. The following section gives different applications of the ANFIS method.

### 1. Control Systems

ANFIS plays a pivotal role in control systems, where precise regulation of processes is vital for optimal performance [25]. In industrial settings, ANFIS models are deployed to dynamically adjust control parameters in response to real-time data feedback. For instance, in manufacturing plants, ANFIS ensures that production processes operate efficiently by fine-tuning parameters such as temperature, pressure, and flow rates [26]. Similarly, in automotive control systems, ANFIS contributes to enhancing vehicle performance and safety by optimizing engine parameters, brake systems, and stability control mechanisms [27, 28]. Moreover, in robotics, ANFIS-based controllers enable robots to adapt their behavior to varying environmental conditions, facilitating tasks such as trajectory planning, grasping objects, and navigating obstacles with precision and agility [29].

### 2. Pattern Recognition

Pattern recognition is a fundamental task in various fields, including speech recognition, handwriting recognition, and image processing. ANFIS excels in this domain due to its ability to handle complex and ambiguous data patterns effectively. In speech recognition applications, ANFIS models analyze speech signals to identify phonemes, words, and sentences, enabling accurate transcription and interpretation of spoken language [30, 31]. Similarly,

in handwriting recognition, ANFIS algorithms decipher handwritten characters and symbols, facilitating text recognition in documents and digital interfaces [32, 33]. Moreover, in image processing tasks such as object detection and classification, ANFIS-based approaches leverage fuzzy logic to interpret visual data and extract meaningful features, contributing to advancements in computer vision and pattern analysis [34].

### 3. Time-Series Prediction

Time-series prediction is crucial in various domains, including finance, weather forecasting, and stock market analysis. ANFIS models excel in this area by leveraging historical data to forecast future trends and outcomes. In finance, ANFIS-based algorithms analyze market data, economic indicators, and investor sentiment to predict stock prices, currency exchange rates, and market indices [35, 36]. These predictions aid investors, traders, and financial institutions in making informed decisions about asset allocation, risk management, and portfolio optimization. Similarly, in weather forecasting, ANFIS models assimilate meteorological data, satellite imagery, and atmospheric conditions to predict temperature, precipitation, and weather patterns with high accuracy [37]. These forecasts are invaluable for disaster preparedness, agriculture, transportation, and other sectors reliant on weather-sensitive activities.

### 4. Fault Detection and Diagnosis

ANFIS is instrumental in fault detection and diagnosis across industrial systems. ANFIS adaptability allows it to generalize across different equipment types and environmental conditions, offering robust fault detection and diagnosis capabilities crucial for maintaining operational reliability and efficiency in diverse industrial settings. For instance, in a manufacturing plant, ANFIS can analyze sensor data from machinery to detect abnormal vibrations indicative of potential bearing wear or misalignment, thus pre-empting breakdowns and optimizing production uptime [38]. In a power distribution network, ANFIS can identify irregularities in voltage or current levels, signalling potential faults such as line overloads or equipment failures, enabling swift intervention to prevent widespread outages [39]. Moreover, ANFIS can be utilized for identifying and diagnosing various issues in solar PV systems [40]. For instance, by analyzing voltage and current data, ANFIS can

detect potential issues such as shading on solar panels, which might manifest as abnormal voltage drops or current fluctuations. Additionally, ANFIS can utilize temperature data to identify overheating components, such as inverters or junction boxes, indicating potential faults or degradation. Also, ANFIS can detect anomalies in irradiance levels, which could signify shading from nearby objects or degradation of solar panels. By integrating these data points and employing fuzzy logic, ANFIS can accurately diagnose the root causes of these issues, whether it is dust accumulation, module degradation, or electrical faults, enabling timely intervention and maintenance to ensure optimal performance and longevity of the solar PV system.

## IV. DATA ACQUISITION AND METHODOLOGY

This section provides a methodology used for this research. The ANFIS was implemented for defect detection and classification based on EL imaging. The main idea is to develop a classification technique that can be utilized in the preventive maintenance of solar farms where the EL camera attached to a drone is used to perform surveys. The EL camera captures the pictures of the solar panels and the smaller solar cells that make up the module. The captured EL images of the solar cells will then be sent through the trained classification algorithm to detect and classify different types of defects on the solar panels. This research focuses on training and validating the detection and classification model that can be utilized for the above-explained procedure. In this research work, solar cells were used for the experiments, and artificial defects (shadows) were created to generate the data sets. Artificial defects were used since these defects can be used as the representation of the actual defects for demonstration purposes. **Table I** provides the specifications of the solar cells used.

TABLE I  
SPECIFICATIONS OF THE SOLAR CELLS USED.

Specification	Value
Max power	4.67 W
Open-circuit voltage	0.645 V
Short-circuit current	8.99 A
Fill Factor	0.81
Efficiency	19 %
Number of busbars	4
Size	156 mm X 156 mm
Technology	Polycrystalline

The artificial defects were created by covering a portion of the solar cell surface using a cardboard mask made from aluminium. The covered portions were then not able to produce the current and because of that, the solar cell is considered defective. Six types of artificial defects were created using this method. **Table II** gives the artificial defects with defect number 0 representing the original solar cell without any defect. The original solar cell was included in this regard for standardization purposes. **Figure 8** shows pictures of different types of shadows for creating artificial defects.

TABLE II  
TYPES OF ARTIFICIAL DEFECTS.

Defect code	Description
0	Original solar cell with no defect.
1	A defect was created by covering the top edge of the solar cell with a long horizontal cardboard mask.
2	A defect was created by covering the side edge of the solar cell with a long vertical cardboard mask
3	A defect was created by placing a big circular cardboard mask at the center of the solar cell.
4	A defect was created by placing a small circular cardboard mask at the center of the solar cell.
5	A defect was created by placing two small circular cardboard masks at the adjacent corners of the solar cell.
6	A defect was created by placing a big circular cardboard mask at the corner of the solar cell.

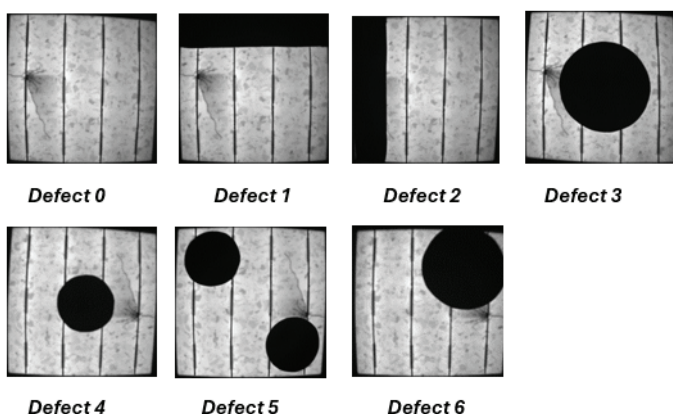


Fig. 8. Different types of shadows (artificial defects)

The experiments to collect the datasets were done indoors, in the laboratory. The procedure for creating the datasets was as follows. A solar cell was placed at the bottom of the isolated box. After that, a specific artificial defect was introduced by

placing an aluminium cardboard on the surface of the solar cell. An InGaAs C12741-0 silicon detector camera was then used to capture the EL image of the defective solar cell. Another different artificial defect was introduced, and the procedure was repeated for all types of defects mentioned above. This process is also repeated with different solar cells and a total of 588 datasets were generated. Thus, the datasets include the EL images and defect code.

### A. EL Images Feature Extraction

As explained in the previous section, every dataset goes with an EL image. Firstly, the quality of the images was improved by removing dead pixels, adjusting the brightness, and fixing the distortion caused by the lens of the camera. In machine learning, it is not easy to directly use EL images to train the models. It is therefore recommended to extract some useful features from the images and then use those features to train the models. To extract the features from the EL images, a histogram of each image was computed in MATLAB. The histogram is a graphical representation of the distribution of pixel intensity values in the image. It shows how many pixels have each intensity value. **Figure 9** shows a typical solar cell with no defect with its respective histogram. The distribution of the histogram has different meanings, the x-axis represents the range of pixel values (intensity), and the y-axis represents the number of pixels at each intensity level. In each histogram, there were two main peaks (one on the left side of the graph and another on the right side), that represent the white (regions of the solar cells that emit more light to the camera) and dark areas (regions of the solar cells that emit less light to the camera) in an EL image. In this research work, the x-axis of the histogram was standardized and kept constant, and the main focus was on the changes in the y-axis of the graph. The values of the two main peaks (Peak 1 and Peak 2), the y-axis standard deviation (Y-STD), and the y-axis median (Y-Median) were extracted from the histogram for use in training the ANFIS model. Peak 1 represents the highest peak in the graph and Peak 2 represents the lower peak on the other side, as shown in **Figure 9**. The standard deviation measures how spread the intensity values are around the mean. In the context of EL images, they indicate the variability in the luminescence across different regions of the solar cells. The median provides the midpoint of the intensity values, offering a robust measure less affected by extreme values (outliers) than the mean.

This is particularly useful in EL imaging, where the distribution of intensity values can be non-normal due to the presence of defective areas.

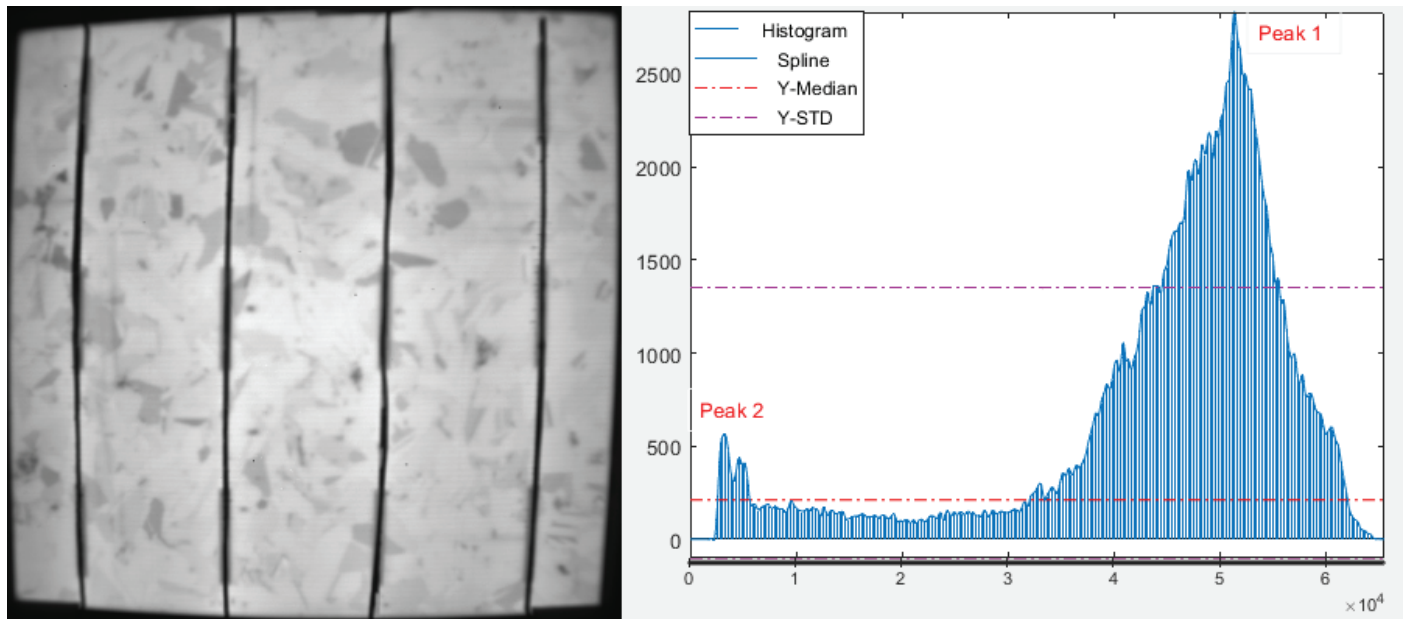


Fig. 9. Typical EL image of a solar cell and its respective histogram

## V. ANFIS IMPLEMENTATION

The input variables to the ANFIS model were the extracted features from the EL images (Peak 1, Peak 2, Y-Median, and Y-STD) and the output variable was the defect code. The design and modeling of the ANFIS model was done in MATLAB. The data were then grouped into three categories, training data (80%) (470 datasets), validation data (10%) (59 datasets), and testing data (10%) (59 datasets). The Sugeno fuzzy inference system (FIS) in MATLAB was used in this study. **Figure 10** below shows the ANFIS model architecture and **Table III** gives the specifications of the ANFIS model.

TABLE III  
 SPECIFICATIONS OF THE ANFIS MODEL.

Parameter	Value/Type
Fuzzy inference system (FIS) type	Sugeno
Inputs	4
Output	1
Membership functions type	Gaussian
FIS generation	Grid partition
Training optimization method	hybrid
Number of Epochs	50
Number of fuzzy rules	24

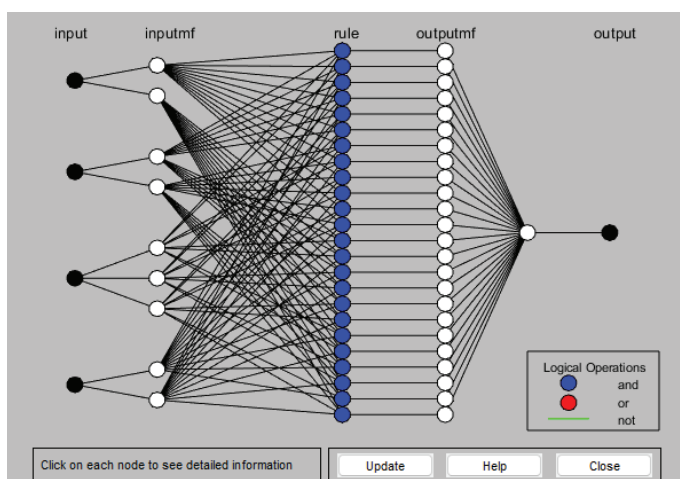


Fig. 10. ANFIS model architecture

Because of the number of the input variables, the Sugeno FIS type was utilized and after several test runs, the Gaussian membership functions were chosen for all input variables. The output variable was set at linear. **Figures 11 and 12** show the membership representation of the FIS variables. The membership functions were designed using the grid partition method and 24 rules were created.



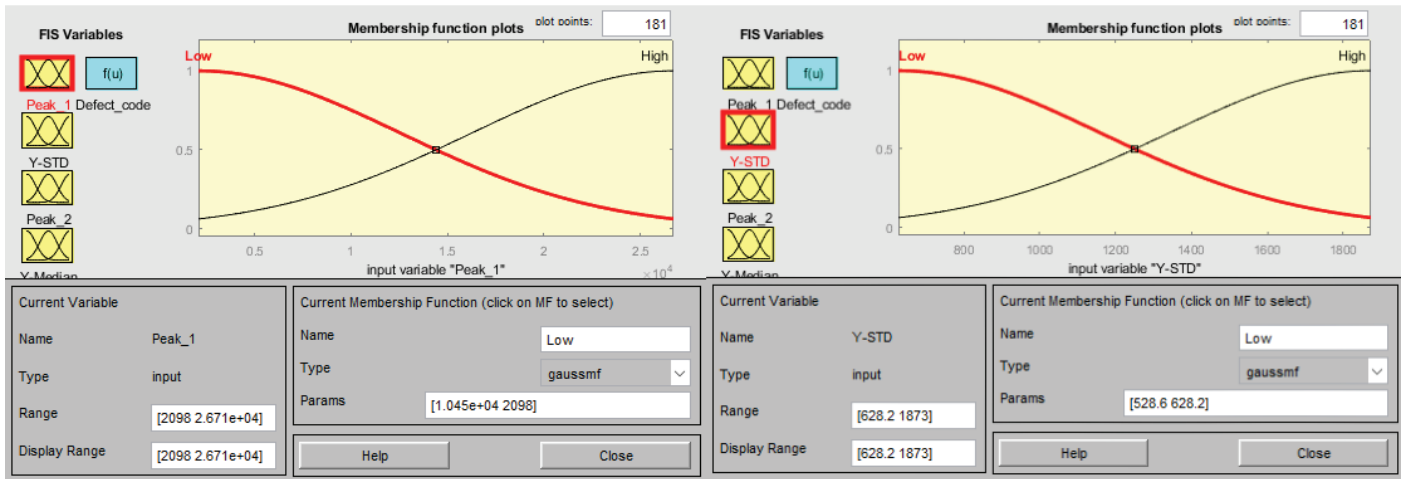


Fig. 11. Membership functions for Peak 1 (left) and Y-STD (right)

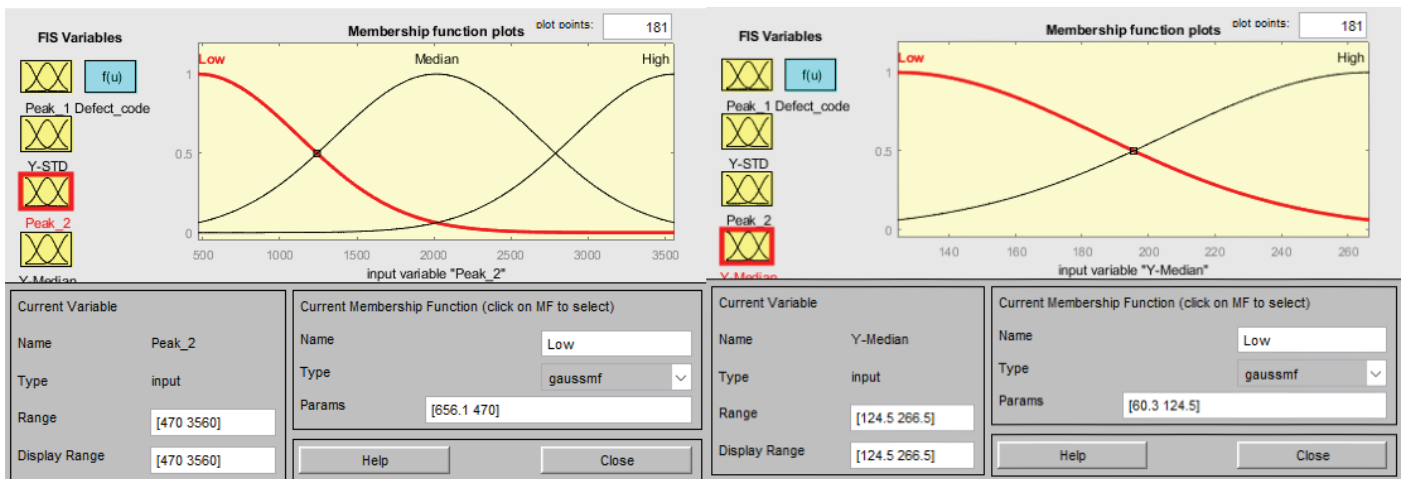


Fig. 12. Membership functions for Peak 2 (left) and Y-Median (right)

After designing the ANFIS model, the training data were loaded. The training data were made up of 470 datasets. The model was then trained using a hybrid optimization training method. The hybrid method combines the backpropagation for the parameters associated with the input membership functions and the least squares estimation for the parameters associated with the output membership

functions. After training, the model was validated and tested to evaluate its performance. In MATLAB, a surface viewer plots the 3D relationship between the variables in an ANFIS model. The shape of the surface indicates how the input variables are related to the output variable. **Figures 13 and 14** show the surface viewer of the input variables and the output variable.

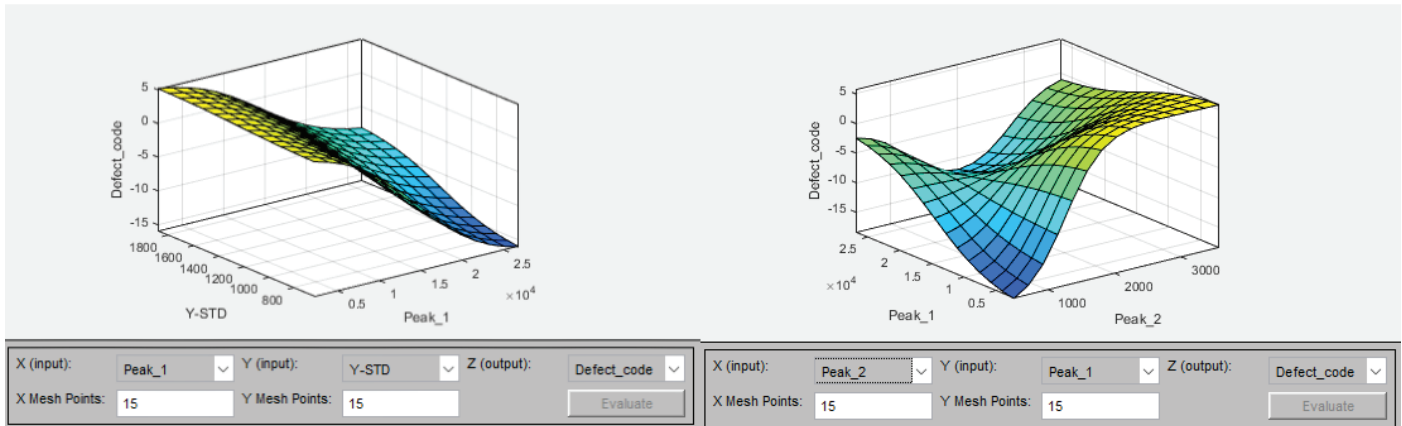


Fig. 13. 3D Surface viewer for Peak 1, Y-STD (left) and Peak 1, Peak 2 (right) against Defect code

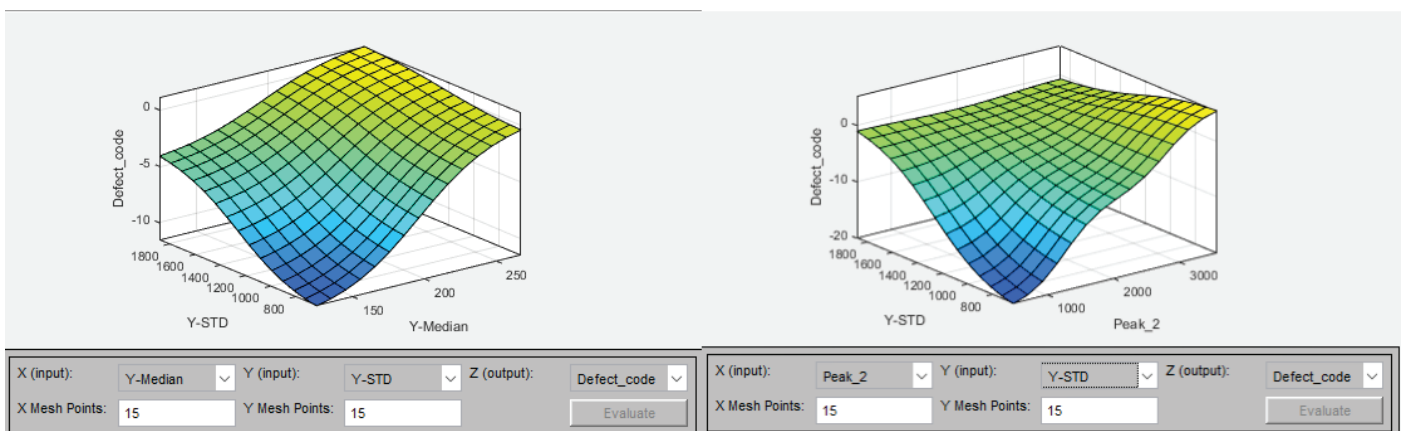


Fig. 14. 3D Surface viewer for Y-Median, Y-STD (left), and Y-STD, Peak 2 (right) against Defect code

## VI. RESULTS AND DISCUSSION

The RMSE was used to evaluate the training, validation, and testing processes during the development of the ANFIS model. For evaluating the predicting accuracy of the model, the coefficient of determination ( $R^2$ ) was used.  $R^2$  is a statistical measure representing the proportion of the variance in the dependent variable that is predictable from the independent variables in a regression model. It is a key metric used to evaluate the goodness-of-fit of a regression model.  $R^2$  typically ranges from 0 to 1 of which a value closer to 1 indicates that a larger proportion of the variance in the dependent variable is explained by the independent variables, suggesting a better fit of the model and it can also be expressed as a percentage. The above-mentioned statistical indicators are given by the following equations,

$$RMSE = \sqrt{\frac{1}{n} \sum_{i=1}^n \{Y_p(i) - Y_a(i)\}^2} \tag{1}$$

where,  $n$  is the sample size,  $Y_p(i)$  represents predicted values and,  $Y_a(i)$  represents the actual values.

$$R^2 = 1 - \frac{RSS}{TSS} \tag{2}$$

where  $RSS$  is the sum of squares of residuals and  $TSS$  represents the total sum of squares. The training of the ANFIS model was evaluated using the RMSE and a value of 0.0519 was obtained. This low RMSE indicates good performance of the model in capturing the patterns present in the training data. However, a very low training RMSE might suggest that the model is overfitting the training data, meaning it learns the noise and specific patterns in the training data rather than the underlying relationships. To avoid overfitting and tune the model hyperparameters, a separate validation dataset was introduced, and a validation RMSE of 0.0947 was obtained. The small difference between the training RMSE and validation RMSE suggests that the model

is generalizing well and is not overfitting the training data. Overfitting would typically result in a much larger gap between training and validation errors. The test dataset was also utilized to evaluate the model's performance after training was complete. These are the data that have not been seen by the model during training and validation. The test RMSE of 0.1100 as obtained during this process. Overall, the test RMSE of 0.1100, following training and validation RMSEs of 0.0519 and 0.0947, respectively, indicates a well-performing and reliable model with good generalization capabilities.

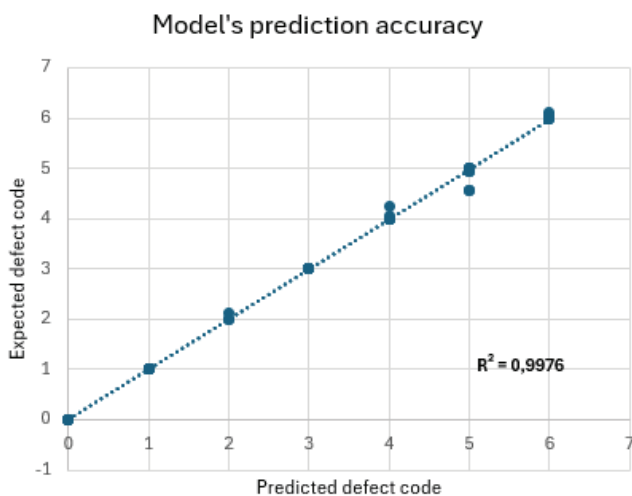


Fig. 15. Prediction accuracy of the model

The model was also evaluated for classification accuracy. This was achieved by utilizing the "evalfis" function in MATLAB to predict the defect code class using the developed model and based on the inputs of the test data. The model predicted defect code was then compared to the original/expected defect code for each test dataset by plotting the model defect code against the original defect code to check the prediction accuracy. The coefficient of determination of 0.9976 was obtained, which translates to a predicting accuracy of 99.76%. This implies that the developed model is highly effective at making accurate predictions on the given dataset. **Figure 15** shows the predicting accuracy of the proposed technique. The proposed method was also compared to other common artificial intelligence techniques used for defect detection and classification of PV cells based on EL imaging as reported in the literature. The comparison was based on the prediction accuracy. **Table IV** compares the proposed technique and other AI methods used for defect detection and classification of PV cells. The proposed technique proves to be among the best for

tackling this problem. However, it should be noted that the dataset sizes are different for techniques compared in **Table IV**.

TABLE IV  
COMPARISON OF THE DESIGNED ANFIS MODEL WITH OTHER AI TECHNIQUES.

Technique	Reference	Datasets size	Accuracy
ANFIS	Present study	588	99.76%
Convolutional neural networks (CNN)	[41]	2624	93.02%
Hybrid fuzzy convolution neural network	[42]	5000	88.38%
Fuzzy logic	[43]	200	97.08%
Support vector machine (SVM)	[44]	200	95.00%
CNN (ResNet-50)	[8]	17064	95.40%
Generative adversarial networks (GAN)	[45]	781	90.00%
Deep neural networks (DNN)	[46]	2624	98.05%
Support Vector Machine	[47]	753	99.70%

## VII. FUTURE WORK AND RECOMMENDATIONS

This research work demonstrates how powerful the ANFIS is for defect detection and classification of solar cells. Future research should investigate the use of more sophisticated image processing algorithms to enhance the quality of EL images, such as noise reduction, contrast enhancement, and defect feature extraction. Integrating deep learning-based image processing techniques could further improve the accuracy and robustness of defect detection and classification. Additionally, developing methods to process high-resolution EL images in real time will allow for more precise defect detection. Optimizing the algorithm for real-time processing is also essential.

Expanding the dataset to include a wider variety of defects and a larger number of EL images is also crucial for improving the training and validation of the neuro-fuzzy system. This dataset should also include images captured under different operating conditions and from different PV cell technologies to ensure the system generalizability. Implementing adaptive learning mechanisms will allow the neuro-

fuzzy system to continuously update itself with new data, enhancing its performance over time. Additionally, developing online learning capabilities will enable the system to learn from new defects and operational scenarios without the need for complete retraining.

Exploring the combination of EL imaging with other imaging techniques, such as infrared (IR) imaging or photoluminescence (PL) imaging, could also improve defect detection and classification accuracy. A multi-modal approach where data from multiple imaging techniques are fused could provide a more comprehensive defect analysis. These advancements will contribute to a more robust and effective defect detection and classification system for solar PV cells.

Future work should also explore applying the ANFIS approach to large-scale operational settings since it may present challenges such as computational complexity, increased training time, and large memory requirements. The computational complexity of ANFIS can be significant, especially when dealing with large datasets or high-dimensional data. As the number of input variables increases, the training time and memory requirements grow exponentially, leading to potential issues with scalability and efficiency. This challenge is compounded by the risk of rule explosion, where the number of fuzzy rules becomes unmanageable, making the system difficult to implement and maintain in real-time operational settings.

Addressing the outlined future work and recommendations will enhance the ANFIS capabilities for solving the problem at hand, ensuring its practical applicability, and contributing to the advancement of defect detection technologies in the solar PV industry. These advancements are crucial

for achieving Sustainable Development Goals related to clean and sustainable energy. By focusing on these areas, the research can continue to evolve, providing more robust, efficient, and practical solutions for defect detection and classification of solar PV cells using EL Imaging, ultimately supporting global efforts toward a sustainable future.

## VIII. CONCLUSION

In conclusion, this research provides a comprehensive investigation into the application of an innovative Adaptive Neuro-Fuzzy Inference System (ANFIS) framework for defect detection and classification of solar PV cells. By harnessing the combined strengths of neural networks and fuzzy logic, the proposed scheme demonstrates a notable capacity to effectively identify and categorize various types of defects encountered in solar photovoltaic systems. The defect detection and classification were performed based on EL imaging. The results showed that the ANFIS is capable of detecting and classifying solar PV cell defects with high accuracy. As for future endeavors, expanding the dataset to encompass a wider array of defect types and environmental conditions could enrich the model learning capacity and improve its robustness in real-world scenarios. Moreover, exploring the integration of advanced sensing technologies and real-time monitoring systems holds the potential for enhancing the proactive detection and mitigation of defects, thereby propelling forward the performance and sustainability of solar PV technologies. This avenue of research not only promises advancements in defect detection methodologies but also contributes significantly to the broader goal of advancing renewable energy systems toward greater reliability and sustainability.

## References

- [1] M. Victoria *et al.*, "Solar photovoltaics is ready to power a sustainable future," 2021. doi: 10.1016/j.joule.2021.03.005.
- [2] M. Alajmi, S. Aljahdali, S. Alsaheel, M. Fattah, and M. Alshehri, "Machine learning as an efficient diagnostic tool for fault detection and localization in solar photovoltaic arrays," 2019. doi: 10.29007/34bz.
- [3] G. Goudelis, P. I. Lazaridis, and M. Dhimish, "A Review of Models for Photovoltaic Crack and Hotspot Prediction," 2022. doi: 10.3390/en15124303.
- [4] B. Doll *et al.*, "Photoluminescence for Defect Detection on Full-Sized Photovoltaic Modules," *IEEE J Photovolt*, vol. 11, no. 6, 2021, doi: 10.1109/JPHOTOV.2021.3099739.

- [5] S. Mohammed, B. Boumediene, and B. Miloud, "Assessment of PV modules degradation based on performances and visual inspection in Algerian Sahara," *International Journal of Renewable Energy Research*, vol. 6, no. 1, 2016, doi: 10.20508/ijrer.v6i1.3155.g6765.
- [6] L. López-Fernández, S. Lagüela, J. Fernández, and D. González-Aguilera, "Automatic evaluation of photovoltaic power stations from high-density RGB-T 3D point clouds," *Remote Sens (Basel)*, vol. 9, no. 6, 2017, doi: 10.3390/rs9060631.
- [7] S. Deitsch *et al.*, "Automatic classification of defective photovoltaic module cells in electroluminescence images," *Solar Energy*, vol. 185, 2019, doi: 10.1016/j.solener.2019.02.067.
- [8] J. Fioresi *et al.*, "Automated Defect Detection and Localization in Photovoltaic Cells Using Semantic Segmentation of Electroluminescence Images," *IEEE J Photovolt*, vol. 12, no. 1, 2022, doi: 10.1109/JPHOTOV.2021.3131059.
- [9] S. Kaplanis, E. Kaplani, and P. N. Borza, "PV Defects Identification through a Synergistic Set of Non-Destructive Testing (NDT) Techniques," *Sensors*, vol. 23, no. 6, 2023, doi: 10.3390/s23063016.
- [10] M. Israil, "Non-destructive Microcracks Detection Techniques in Silicon Solar Cell," *Physical Science International Journal*, vol. 4, no. 8, 2014, doi: 10.9734/psij/2014/8754.
- [11] R. Ebner, B. Kubicek, and G. Ujvari, "Non-destructive techniques for quality control of PV modules: Infrared thermography, electro- and photoluminescence imaging," in *IECON Proceedings (Industrial Electronics Conference)*, 2013. doi: 10.1109/IECON.2013.6700488.
- [12] G. C. Eder, Y. Voronko, C. Hirschl, R. Ebner, G. Újvári, and W. Mühleisen, "Non-destructive failure detection and visualization of artificially and naturally aged PV modules," *Energies (Basel)*, vol. 11, no. 5, 2018, doi: 10.3390/en11051053.
- [13] M. Sander, B. Henke, S. Schweizer, M. Ebert, and J. Bagdahn, "PV module defect detection by combination of mechanical and electrical analysis methods," in *Conference Record of the IEEE Photovoltaic Specialists Conference*, 2010. doi: 10.1109/PVSC.2010.5615878.
- [14] H. P. C. Hwang, C. C. Y. Ku, and J. C. C. Chan, "Detection of malfunctioning photovoltaic modules based on machine learning algorithms," *IEEE Access*, vol. 9, 2021, doi: 10.1109/ACCESS.2021.3063461.
- [15] R. A. Eltuhamy, M. Rady, E. Almatrafi, H. A. Mahmoud, and K. H. Ibrahim, "Fault Detection and Classification of CIGS Thin-Film PV Modules Using an Adaptive Neuro-Fuzzy Inference Scheme," *Sensors*, vol. 23, no. 3, 2023, doi: 10.3390/s23031280.
- [16] H. Yang, W. He, H. Wang, J. Huang, and J. Zhang, "Assessing power degradation and reliability of crystalline silicon solar modules with snail trails," *Solar Energy Materials and Solar Cells*, vol. 187, 2018, doi: 10.1016/j.solmat.2018.07.021.
- [17] S. Kajari-Schröder, I. Kunze, and M. Köntges, "Criticality of cracks in PV modules," in *Energy Procedia*, 2012. doi: 10.1016/j.egypro.2012.07.125.
- [18] M. Dhimish and A. M. Tyrrell, "Power loss and hotspot analysis for photovoltaic modules affected by potential induced degradation," *Npj Mater Degrad*, vol. 6, no. 1, 2022, doi: 10.1038/s41529-022-00221-9.
- [19] A. A. Q. Hasan, A. A. Alkahtani, S. A. Shahahmadi, M. N. E. Alam, M. A. Islam, and N. Amin, "Delamination-and electromigration-related failures in solar panels—a review," *Sustainability (Switzerland)*, vol. 13, no. 12, 2021, doi: 10.3390/su13126882.
- [20] K. moh Lin *et al.*, "Detection of soldering induced damages on crystalline silicon solar modules fabricated by hot-air soldering method," *Renew Energy*, vol. 83, 2015, doi: 10.1016/j.renene.2015.05.017.
- [21] M. Demant *et al.*, "Micro-Cracks in Silicon Wafers and Solar Cells: Detection and Rating of Mechanical Strength and Electrical Quality," *29th European PV Solar Energy Conference*

and Exhibition, no. September, 2014.

- [22] R. Tabbussum and A. Q. Dar, "Performance evaluation of artificial intelligence paradigms—artificial neural networks, fuzzy logic, and adaptive neuro-fuzzy inference system for flood prediction," *Environmental Science and Pollution Research*, vol. 28, no. 20, 2021, doi: 10.1007/s11356-021-12410-1.
- [23] P. J, V. K, M. B, P. M, and U. R, "Prediction of Air Pollution Utilizing an Adaptive Network Fuzzy Inference System with the Aid of Genetic Algorithm," *Nat Eng Sci*, vol. 9, no. 1, pp. 46–56, May 2024, doi: 10.28978/nesciences.1489228.
- [24] Bukya Ravi, Mohan G. Madhu, and Sharanya M., "Simulation and Implementation of PI, Fuzzy and ANFIS Controller for PV and WIND Based EV Charging Station," 2024, doi: <https://doi.org/10.21203/rs.3.rs-4221312/v1>.
- [25] A. Kusagur, S. F. Kodad, and B. V. S. Ram, "Modeling, Design and Simulation of an Adaptive Neuro-Fuzzy Inference System (ANFIS) for Speed Control of Induction Motor," *Int J Comput Appl*, vol. 6, no. 12, 2010, doi: 10.5120/1123-1472.
- [26] M. Al-Mahasneh, M. Aljarrah, T. Rababah, and M. Alu'datt, "Application of Hybrid Neural Fuzzy System (ANFIS) in Food Processing and Technology," 2016. doi: 10.1007/s12393-016-9141-7.
- [27] M. A. George, D. V. Kamat, and C. P. Kurian, "Electric vehicle speed tracking control using an ANFIS-based fractional order PID controller," *Journal of King Saud University - Engineering Sciences*, vol. 36, no. 4, 2024, doi: 10.1016/j.jksues.2022.01.001.
- [28] M. Suhail, I. Akhtar, S. Kirmani, and M. Jameel, "Development of Progressive Fuzzy Logic and ANFIS Control for Energy Management of Plug-In Hybrid Electric Vehicle," *IEEE Access*, vol. 9, 2021, doi: 10.1109/ACCESS.2021.3073862.
- [29] M. Lazreg and N. Benamrane, "Hybrid system for optimizing the robot mobile navigation using ANFIS and PSO," *Rob Auton Syst*, vol. 153, 2022, doi: 10.1016/j.robot.2022.104114.
- [30] I. Balabanova and G. Georgiev, "Speech Profile Recognition by Fourier Spectral, FFNN and ANFIS Techniques," in *29th National Conference with International Participation, TELECOM 2021 - Proceedings*, 2021. doi: 10.1109/TELECOM53156.2021.9659793.
- [31] J. Nassr Nassr, I. Ighneiwa Ighneiwa, O. elbadri elbadri, and Z. Rajab Hasan, "Using Neuro-Fuzzy System to Improve Speech Recognition," in *The 7th International Conference on Engineering & MIS 2021*, New York, NY, USA: ACM, Oct. 2021, pp. 1–8. doi: 10.1145/3492547.3492755.
- [32] Naidu U. Ganesh, Thiruvengatanadhan R., Narayana S, Sivaprakasam T., and Dhanalakshmi P., "Improved Adaptive Neuro Fuzzy Inference System for Handwritten Optical Character Recognition," 2020, doi: DOI: 10.34218/IJARET.11.11.2020.073.
- [33] Chen Dewang, Wang Xin, Yuqi Lu, Du Hongqing, Marano Giuseppe Carlo, and Hung José Romero, "Deep Neural Fuzzy Systems with High Robustness and Strong Interpretability for Handwriting Recognition with Different Gaussian Noises," *Available at SSRN 4603169*, 2023, doi: <http://dx.doi.org/10.2139/ssrn.4603169>.
- [34] V. Cynthia Dewi, V. Amrizal, and F. Eka Muzayyana Agustin, "Implementation of Adaptive Neuro-Fuzzy Inference System and Image Processing for Design Applications Paper Age Prediction," *Jurnal Riset Ilmu Teknik*, vol. 1, no. 1, 2023, doi: 10.59976/jurit.v1i1.6.
- [35] F. Ghashami and K. Kamyar, "Performance Evaluation of ANFIS and GA-ANFIS for Predicting Stock Market Indices," *Int J Econ Finance*, vol. 13, no. 7, 2021, doi: 10.5539/ijef.v13n7p1.
- [36] W. Hussain, J. M. Merigó, and M. R. Raza, "Predictive intelligence using ANFIS-induced OWAWA for complex stock market prediction," *International Journal of Intelligent Systems*, vol. 37, no. 8, 2022, doi: 10.1002/int.22732.
- [37] V. X. C. Del Rosario, V. J. Narca, F. T. J. Laconsay, and C. J. Alliac, "Weather Forecasting Rain Probability in Cebu Using ANFIS and Bayesian Network," in *Proceedings - 2021 1st International Conference in Information and*

- Computing Research, iCORE 2021*, 2021. doi: 10.1109/iCORE54267.2021.00026.
- [38] Y. Lei, Z. He, Y. Zi, and Q. Hu, "Fault diagnosis of rotating machinery based on multiple ANFIS combination with GAs," *Mech Syst Signal Process*, vol. 21, no. 5, 2007, doi: 10.1016/j.ymsp.2006.11.003.
- [39] A. A. Elbaset and T. Hiyama, "Fault detection and classification in transmission lines using ANFIS," *IEEJ Transactions on Industry Applications*, vol. 129, no. 7, 2009, doi: 10.1541/ieejias.129.705.
- [40] A. F. Bendary, A. Y. Abdelaziz, M. M. Ismail, K. Mahmoud, M. Lehtonen, and M. M. F. Darwish, "Proposed anfis based approach for fault tracking, detection, clearing and rearrangement for photovoltaic system," *Sensors*, vol. 21, no. 7, 2021, doi: 10.3390/s21072269.
- [41] M. W. Akram *et al.*, "CNN based automatic detection of photovoltaic cell defects in electroluminescence images," *Energy*, vol. 189, 2019, doi: 10.1016/j.energy.2019.116319.
- [42] W. Tang, Q. Yang, and W. Yan, "Deep Learning-Based Algorithm for Multi-Type Defects Detection in Solar Cells with Aerial EL Images for Photovoltaic Plants," *CMES - Computer Modeling in Engineering and Sciences*, vol. 130, no. 3, 2022, doi: 10.32604/cmcs.2022.018313.
- [43] W. Junchao and Z. Chang, "Defect detection on solar cells using mathematical morphology and fuzzy logic techniques," *Journal of Optics (India)*, vol. 53, no. 1, 2024, doi: 10.1007/s12596-023-01162-5.
- [44] R. O. Serfa Juan and J. Kim, "Photovoltaic Cell Defect Detection Model based-on Extracted Electroluminescence Images using SVM Classifier," in *2020 International Conference on Artificial Intelligence in Information and Communication, ICAIIC 2020*, 2020. doi: 10.1109/ICAIIIC48513.2020.9065065.
- [45] C. Shou *et al.*, "Defect detection with generative adversarial networks for electroluminescence images of solar cells," in *Proceedings - 2020 35th Youth Academic Annual Conference of Chinese Association of Automation, YAC 2020*, 2020. doi: 10.1109/YAC51587.2020.9337676.
- [46] H. Munawer Al-Otum, "Deep learning-based automated defect classification in Electroluminescence images of solar panels," *Advanced Engineering Informatics*, vol. 58, 2023, doi: 10.1016/j.aei.2023.102147.
- [47] C. Mantel *et al.*, "Machine learning prediction of defect types for electroluminescence images of photovoltaic panels," 2019. doi: 10.1117/12.2528440.